Frequency Response Analysis of General Zero-Crossing Reset Control Systems

van Eijk, Luke F.; Kostić, Dragan; HosseinNia, S. Hassan

DOI
10.1109/LCSYS.2025.3581185

Publication date
2025

Document Version
Final published version

Published in
IEEE Control Systems Letters

Frequency Response Analysis of General Zero-Crossing Reset Control Systems

Luke F. van Eijk, Dragan Kostić, and S. Hassan HosseinNia, *Senior Member, IEEE*

***Abstract*—This letter introduces an output prediction method for a general class of closed-loop reset control systems. The considered type of system consists of a linear time-invariant (LTI) part which is connected in feedback with a reset controller that (partially) resets (a part of) its states when its input is equal to zero. Given some practical assumptions on the reset element's input signal, the system output can be accurately predicted when the system is subject to a sinusoidal input. One benefit of this approach is that it provides an intuitive frequency-domain representation of the system. Another benefit is that output prediction can be done based solely on a frequency-response function (FRF) of the LTI part of the system. This letter also introduces an accurate and computationally efficient algorithm which can – based on the predicted output – compute a closed-loop pseudo-sensitivity. This pseudo-sensitivity represents the ratio between the maximum absolute value of the system's output and the amplitude of its input, similar to the closed-loop sensitivity functions for LTI systems.**

***Index Terms*—Frequency domain, nonlinear feedback control, reset control.**

I. Introduction

LINEAR control has been of significant importance in a wide variety of applications, ranging from cruise control in cars to trajectory tracking in semiconductor chip manufacturing equipment [1]. When the plant is also linear, a benefit of linear controllers is that they can be intuitively designed in the frequency domain. To this end, the control designer can for example use closed-loop sensitivity functions. These sensitivity functions provide a relation between certain inputs to the system (such as a reference trajectory, external disturbance, or measurement noise) and certain outputs (such as the positioning error, controller output, or plant output) [2]. More specifically, given a sinusoidal input, a sensitivity function can be used to fully accurately predict how much these signals are amplified in a certain output. An additional benefit of this approach is that the sensitivity functions can be constructed using a frequency-response function (FRF) of the plant, which can be obtained based only on a limited amount of measurement data [3]. Therefore, a parametric model of the plant is not required. However, a disadvantage of linear control is that it has inherent performance limitations. These limitations can for example be expressed by means of Bode's sensitivity integral or Bode's gain-phase relationship [4].

Reset control is a nonlinear control technique in which (part of) the controller states are reset to a fraction of the original state when certain conditions are satisfied, such as when the input signal is equal to zero. It has been theoretically proven that reset controllers can overcome certain inherent limitations of linear control, see, e.g., [5], [6]. Even though reset control is not the only technique for which this can be achieved, a benefit of reset control is that there are frequency domain design tools available which are similar to those that are often used for linear control design. Namely, in [7] a methodology has been developed based on which a sensitivity function can be constructed – using only a plant FRF – for closed-loop systems in which resets are triggered when the reset element's input is zero. Given a sinusoidal input, and under the condition that the system converges to a periodic output with the same period as the input signal, the methodology allows to analytically predict what this output looks like. Although the approach makes some practical assumptions on the reset element's input, it has been illustrated through simulations and experiments that this results in an accurate prediction of the periodic output. Subsequently, the (pseudo)sensitivity is defined as the relation between the maximum amplitude of the periodic output with respect to the amplitude of the sinusoidal input. In [8] it has been experimentally shown on an industrial wirebonding machine that, using this methodology, a reset controller can be designed that outperforms a linear controller that is designed using the same constraints on the sensitivity function.

Even though reset control design using the pseudosensitivity shows potential, there are still two limitations hindering wider adoption of this approach. As a first limitation, the methodology in [7] cannot be used if there are additional linear control elements around the reset element, which can help to improve the controller's performance, as shown in, e.g., [9], [10]. An extension has been made in [8] that also

Received 16 March 2025; revised 19 May 2025; accepted 9 June 2025. Date of publication 19 June 2025; date of current version 7 July 2025. This work was supported by ASMPT. Recommended by Senior Editor S. Baldi. *(Corresponding author: Luke F. van Eijk.)*

Luke F. van Eijk is with the Department of Precision and Microsystems Engineering, Delft University of Technology, 2628 CD Delft, The Netherlands, and also with the Center of Competency, ASMPT, 6641 TL Beuningen, The Netherlands (e-mail: L.F.vanEijk@tudelft.nl).

Dragan Kostić is with ASMPT, 6641 TL Beuningen, The Netherlands (e-mail: dragan.kostic@asmpt.com).

S. Hassan HosseinNia is with the Department of Precision and Microsystems Engineering, Delft University of Technology, 2628 CD Delft, The Netherlands (e-mail: S.H.HosseinNiaKani@tudelft.nl).

Digital Object Identifier 10.1109/LCSYS.2025.3581185

allows linear filters before, after, and in parallel to the reset element. However, in [8] the pseudosensitivity can only be computed from the reference trajectory to the error signal. Furthermore, many practical control systems contain multiple loops, such as an internal current control loop and an external position control loop. These systems do not fit into any of the system-classes considered in the existing literature. In other words, there is no general framework which allows to compute the pseudosensitivity from any input to any output, and with a reset element present at any place within the system. As a second limitation, from the existing literature is unclear how to numerically implement the analytical methodology, but it is non-trivial how to do this in a proper way. A primary difficulty is that the plant FRF is in practice not available at all frequencies, but instead only within a finite range of frequencies and with a certain frequency resolution. Furthermore, it is not straightforward to compute the pseudosensitivity in an accurate though computationally efficient manner.

The aim of this letter is to address the two mentioned limitations. First, we develop a method to compute the pseudosensitivity for a system where all the linear elements are combined into one block and are placed in feedback with the reset element. Note that this type of system shows resemblance to the well-known Lure system [11]. Since any system containing linear elements and a reset element can be rewritten into this form, this unifies and extends upon the existing literature. Second, we propose a numerical algorithm to compute the pseudosensitivity, which allows the use of a plant FRF containing data with a finite frequency-range and frequency-resolution. Hereby, focus is also placed on making the algorithm accurate but still computationally efficient.

The remainder of this letter is organized as follows. In Section II, preliminaries on the existing methodology are provided. Subsequently, the extension of the methodology to the more general class of reset control systems is presented in Section III. Next, Section IV illustrates how our work is a generalization of the available literature. In Section V we present the numerical algorithm for computing the pseudosensitivity. Finally, we end with a conclusion in Section VI.

Notation: For a time-domain signal $q(t)$ with time $t \in \mathbb{R}$, its Laplace transform is denoted by the capitalized version $Q(s)$, with Laplace variable $s \in \mathbb{C}$. We say that a periodic signal $r(t)$ with period T has a zero-mean if $\int_{t_0}^{t_0+T} r(t)\mathrm{d}t = 0 \, \forall t_0 \in \mathbb{R}$. The absolute value and angle of a complex number a are denoted by $|a|$ and $\angle a$, respectively. In other words, $a = |a|e^{j\angle a}$, with imaginary unit $j := \sqrt{-1}$. Taking the floor of a real number b is denoted by $\lfloor b \rfloor$. We denote an identity matrix and zero matrix of size m by I_m and 0_m, respectively. For a matrix M, its eigenvalues are denoted by $\lambda(M)$.

II. Preliminaries

A. Definition of the Reset Element

Consider a reset element which is given by

$$R := \begin{cases} \dot{x}(t) = Ax(t) + By(t), & \text{if } y(t) \neq 0, \\ x(t^+) = A_\rho x(t), & \text{if } y(t) = 0, \\ u(t) = Cx(t), \end{cases} \tag{1}$$

with input $y \in \mathbb{R}$, output $u \in \mathbb{R}$, states $x \in \mathbb{R}^m$, state-space matrices $A \in \mathbb{R}^{m\times m}$, $B \in \mathbb{R}^{m\times 1}$, $C \in \mathbb{R}^{1\times m}$, and reset matrix $A_\rho \in \mathbb{R}^{m\times m}$, where $t^+ := \lim_{\tau\to t, \tau>t} \tau$. When $A_\rho = I_m$, the reset element behaves like an LTI system given in the frequency-domain by $U(s) = R_{\mathrm{bl}}(s)Y(s)$, with

$$R_{\mathrm{bl}}(s) = C(sI_m - A)^{-1}B. \tag{2}$$

Without loss of generality, reset element R does not contain a direct feed-through term from input y to output u. Namely, such a feed-through term can be implemented by means of a linear gain in parallel to the reset element. Such an LTI filter can be captured in the LTI part of the system we consider.

B. Response of the Reset Element to a Sinusoidal Input

Consider a reset element which is subject to a sinusoidal input $y(t) = \hat{y}\sin(\omega t + \varphi_y)$, with amplitude $\hat{y} \in \mathbb{R}_{>0}$, phase $\varphi_y \in \mathbb{R}$, and frequency $\omega \in \mathbb{R}_{>0}$. Then, as shown in [12, Proposition 2], the output of the reset element converges to a $\frac{2\pi}{\omega}$-periodic solution if it holds that

$$\left|\lambda\left(A_\rho e^{A\delta}\right)\right| < 1 \quad \forall \delta \in \mathbb{R}_{>0}. \tag{3}$$

In this letter we are interested in reset elements for which this condition is indeed satisfied. A necessary condition for (3) to hold is that reset matrix A_ρ satisfies $|\lambda(A_\rho)| \leq 1$ (see [12, Remark 4]). However, having a stable base-linear system (i.e., A is Hurwitz) is not always necessary. For example, the condition (3) holds for any A if $A_\rho = 0_m$.

Next, note that such a $\frac{2\pi}{\omega}$-periodic output of the reset element (1) can be described by the Fourier series [13]

$$u(t) = \sum_{n=1}^{\infty} |H_n(\omega)|\hat{y}\sin\left(n\left(\omega t + \varphi_y\right) + \angle H_n(\omega)\right), \tag{4}$$

where $H_n \in \mathbb{C}$ contains the magnitude- and phase-characteristics of the n^{th}-order harmonic. These characteristics have been derived in [7, Th. 3.1] and are given by

$$H_n(\omega) = \begin{cases} C(j\omega I_m - A)^{-1}\left(I_m + j\Theta_{\mathrm{D}}(\omega)\right)B, & \text{for } n = 1, \\ C(jn\omega I_m - A)^{-1}j\Theta_{\mathrm{D}}(\omega)B, & \text{for odd } n \geq 2, \\ 0, & \text{for even } n \geq 2, \end{cases} \tag{5}$$

$$\Theta_{\mathrm{D}}(\omega) = \frac{-2\omega^2}{\pi}\Delta(\omega)\left[\Gamma_{\mathrm{r}}(\omega) - \Lambda^{-1}(\omega)\right], \tag{6}$$

$$\Gamma_{\mathrm{r}}(\omega) = \Delta_{\mathrm{r}}^{-1}(\omega)A_\rho\Delta(\omega)\Lambda^{-1}(\omega), \ \Lambda(\omega) = \omega^2 I + A^2, \tag{7}$$

$$\Delta_{\mathrm{r}}(\omega) = I + A_\rho e^{\frac{\pi}{\omega}A}, \ \Delta(\omega) = I + e^{\frac{\pi}{\omega}A}. \tag{8}$$

For later use, note that after rewriting we can also express the Fourier series as

$$u(t) = \sum_{n=1}^{\infty} |U_n(\omega)|\sin\left(n\omega t + \angle U_n(\omega)\right), \tag{9}$$

$$U_n(\omega) = H_n(\omega)Y_1(\omega)e^{j(n-1)\angle Y_1(\omega)}, \tag{10}$$

where $Y_1(\omega) = \hat{y}e^{j\varphi_y}$.

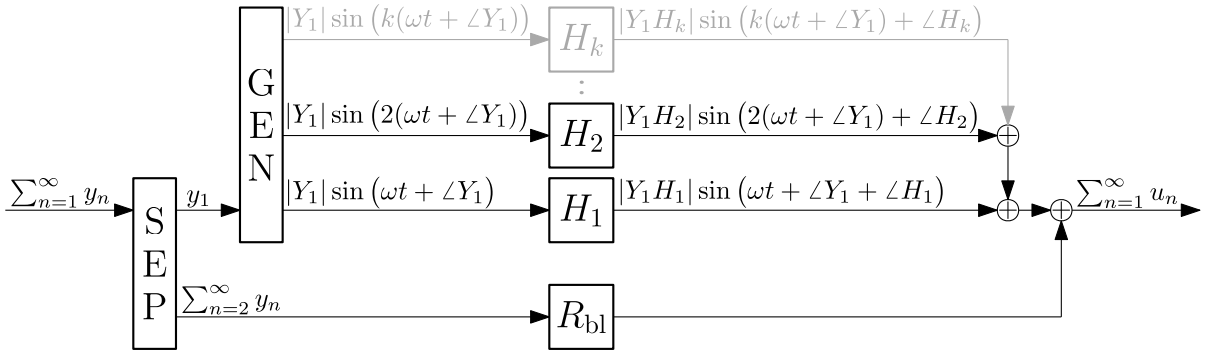

Fig. 1. Visual interpretation of a reset element R subject to a periodic input (11), modeled using the harmonic separator (adapted from [7]).

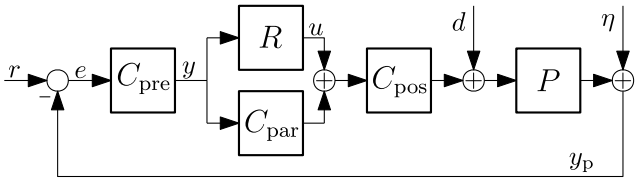

Fig. 2. Schematic representation of a closed-loop system with a reset element R as in (1), and LTI elements C_{pre}, C_{par}, C_{pos}, and P.

C. Response of the Reset Element to a Periodic Input

Consider a reset element which is subject to a $\frac{2\pi}{\omega}$-periodic input, such that it can be described by the Fourier series

$$y(t) = \sum_{n=1}^{\infty} y_n(t), \tag{11}$$

$$y_n(t) = |Y_n(\omega)|\sin\left(n\omega t + \angle Y_n(\omega)\right), \tag{12}$$

with $Y_n \in \mathbb{C}$. Since this is not a pure sinusoidal input, we cannot directly predict the output using the method explained in Section II-B. A pragmatic solution is proposed in [7], where the reset element's behaviour in response to a periodic input (11) is modelled as in Fig. 1. In this model, the higher-order harmonics are separated from the first harmonic and are passed through the reset element's underlying linear dynamics (2). Subsequently, the input-output behaviour of the first harmonic can again be derived as in Section II-B. In that case, the first harmonic of the output is still given by

$$U_1(\omega) = H_1(\omega)Y_1(\omega), \tag{13}$$

in line with (10). However, the higher-order harmonics in the output now also contain the effect of passing the higher-order harmonics at the input through the reset element's underlying linear dynamics, which yields

$$U_n(\omega) = H_n(\omega)Y_1(\omega)e^{j(n-1)\angle Y_1(\omega)} + \cdots \\ R_{\mathrm{bl}}(nj\omega)Y_n(\omega)\,\forall n \neq 1. \tag{14}$$

In view of space considerations, we want to refer the interested reader to [7] for a more detailed explanation about this model.

In [7] and [8], the model from Fig. 1 has been used to predict the stationary behaviour of specific classes of closed-loop reset control systems. To be more specific, consider the system in Fig. 2 with single-input single-output (SISO) LTI plant P, SISO LTI control elements C_{pre}, C_{par}, C_{pos}, and reset element R. The system has three external inputs: reference $r \in \mathbb{R}$, measurement noise $\eta \in \mathbb{R}$, and disturbance $d \in \mathbb{R}$. In [7], a special case of Fig. 2 is considered where $C_{\mathrm{pre}} = 1$, $C_{\mathrm{pos}} = 1$, and $C_{\mathrm{par}} = 0$. Under those conditions, it is possible to compute the stationary response of signals e, u, and y_{p}, when the system is subject to a sinusoidal input in r, d, or η. An important benefit is that only an FRF of the plant is required to compute the stationary responses. In [8], an extension is made by considering the complete system in Fig. 2. However, it is only possible to compute the stationary response of error e under a sinusoidal reference r.

Numerical and experimental validations in [7] suggest that, using the model in Fig. 1, it is possible to accurately predict the closed-loop behaviour when the amplitudes of the higher-order harmonics at the reset element's input y are significantly smaller than the amplitude of the first harmonic, i.e., $|Y_n(\omega)| \ll |Y_1(\omega)|\,\forall n \neq 1$. A pragmatic method to evaluate whether the higher-order harmonics are small enough, is to check whether they cause any additional state-resets. When only the first harmonic is present, this results in two resets per period (at the zero-crossings of the sinusoid). When higher-order harmonics become too large, this can result in more than two zero-crossings per period. The results in [7] suggest that having two resets gives a good indication for the accuracy of the predicted behaviour, whereas the prediction can become less trustworthy when there are more than two resets.

D. Definition of the Pseudosensitivity

Consider a reset control system subject to a sinusoidal external input

$$w(t) = \hat{w}\sin\left(\omega t + \varphi_w\right), \tag{15}$$

with amplitude $\hat{w} \in \mathbb{R}_{>0}$ and phase $\varphi_w \in \mathbb{R}$. This input can for example be a reference or disturbance. The system also has a performance output $z \in \mathbb{R}$ – such as the error – which we assume converges to a unique periodic solution $z_{\mathrm{s}} \in \mathbb{R}$ with period $T = \frac{2\pi}{\omega}$, which is the same period as the sinusoidal input. We can then compute the ratio between the maximum amplitude of the output signal and the amplitude of the input signal, defined as

$$|S_\infty(\omega)| := \frac{\max_{t\in[0,T)} |z_{\mathrm{s}}(t)|}{\hat{w}}. \tag{16}$$

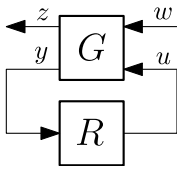

Fig. 3. Schematic representation of a system with an LTI element G as in (17)-(18), placed in feedback with a reset element R as in (1).

This relation is defined as the pseudosensitivity in [14], giving a 'worst-case' measure of the amplification in the output.

III. Main Result

Consider the system in Fig. 3 with reset element R and LTI system G. System G has two inputs; an external input $w \in \mathbb{R}$, and the reset element's output u. It also has two outputs; a performance output $z \in \mathbb{R}$, and the reset element's input y. The input-output relation of the LTI system can be described in the frequency-domain by

$$\begin{bmatrix} Z(s) \\ Y(s) \end{bmatrix} = G(s) \begin{bmatrix} W(s) \\ U(s) \end{bmatrix}, \tag{17}$$

$$G(s) \coloneqq \begin{bmatrix} G_{wz}(s) & G_{uz}(s) \\ G_{wy}(s) & G_{uy}(s) \end{bmatrix}. \tag{18}$$

Definition 1: Consider the system in Fig. 3 with any initial conditions for LTI system G and reset element R, which is subject to a sinusoidal input w as in (15). We call this system *sinusoidal-input convergent* if the signals u, y, and z converge to a unique $\frac{2\pi}{\omega}$-periodic solution with a zero-mean.

In this letter we focus on systems which are sinusoidal-input convergent. We deem this to be reasonable, because for computing a pseudosensitivity it is anyways necessary that the system's output converges to a $\frac{2\pi}{\omega}$-periodic solution. Furthermore, having a zero-mean significantly eases the subsequent derivations and was also required in [7], [8]. Even though it is not the focus of this letter, we want to point the reader towards [14], which provides conditions to check whether a system as in Fig. 3 is sinusoidal-input convergent. Next, we present Theorem 1. For systems that are indeed sinusoidal-input convergent, this theorem provides analytical expressions to describe the periodic solutions to which the performance output and reset element input converge.

Theorem 1: Consider the system in Fig. 3 with LTI system G as in (17)-(18) and reset element R as in (1), both with any initial conditions, subject to a sinusoidal input w as in (15). When 1) the system is sinusoidal-input convergent, 2) the condition in (3) holds, and 3) the reset element is modeled as in Fig. 1, then the reset element's input converges to a periodic solution given by

$$y(t) = \hat{w} \sum_{n=1}^{\infty} |S_{y,n}(\omega)| \sin\big(n(\omega t + \varphi_w) + \angle S_{y,n}(\omega)\big), \tag{19}$$

where the higher-order sinusoidal-input sensitivity functions (HOSISFs) are defined as

$$S_{y,1}(\omega) \coloneqq \frac{G_{wy}(j\omega)}{1 - G_{uy}(j\omega)H_1(\omega)}, \tag{20}$$

$$S_{y,n}(\omega) \coloneqq \frac{G_{uy}(nj\omega)H_n(\omega)S_{y,1}(\omega)e^{j(n-1)\angle S_{y,1}(\omega)}}{1 - G_{uy}(nj\omega)R_{\mathrm{bl}}(nj\omega)} \; \forall n \neq 1. \tag{21}$$

Furthermore, the performance output converges to a periodic solution given by

$$z(t) = \hat{w} \sum_{n=1}^{\infty} |S_{z,n}(\omega)| \sin\big(n(\omega t + \varphi_w) + \angle S_{z,n}(\omega)\big), \tag{22}$$

where the HOSISFs are defined as

$$S_{z,1}(\omega) \coloneqq G_{wz}(j\omega) + G_{uz}(j\omega)H_1(\omega)S_{y,1}(\omega), \tag{23}$$

$$S_{z,n}(\omega) \coloneqq \frac{G_{uz}(nj\omega)H_n(\omega)S_{y,1}(\omega)e^{j(n-1)\angle S_{y,1}(\omega)}}{1 - G_{uy}(nj\omega)R_{\mathrm{bl}}(nj\omega)} \; \forall n \neq 1. \tag{24}$$

Proof: See Appendix. ∎

Several conclusions can be drawn from Theorem 1. First, the theorem provides an intuitive link between closed-loop time- and frequency-domain behaviour of the system, by means of what we call the HOSISFs. Second, in turn, the HOSISFs provide an intuitive link between the open- and closed-loop frequency-domain behaviour of the system, which can be used for reset control design purposes. For a more intuitive explanation on how harmonics are generated by the reset element and how they flow through the closed-loop system, we refer the reader to [7]. Third, note that this method allows to predict the time-domain solution based purely on the FRF of LTI system G. Finally, we again want to stress that any closed-loop system containing a reset element R and various LTI elements, can be rewritten into the form in Fig. 3. We will illustrate this is the next section.

IV. Illustrative Example

As an example, we use Theorem 1 to derive the HOSISFs from reference r to error e for the system in Fig. 2. These HOSISFs have also specifically been derived in [8]. As a first step, we transform the system into the form of Fig. 3 with external input $w = r$ and performance output $z = e$ (under the assumption that $d = 0$ and $\eta = 0$). This yields the LTI system G as in (17)-(18) with

$$G_{wz}(s) = \frac{1}{1 + P(s)C_{\mathrm{pos}}(s)C_{\mathrm{par}}(s)C_{\mathrm{pre}}(s)}, \tag{25}$$

$$G_{uz}(s) = \frac{-P(s)C_{\mathrm{pos}}(s)}{1 + P(s)C_{\mathrm{pos}}(s)C_{\mathrm{par}}(s)C_{\mathrm{pre}}(s)}, \tag{26}$$

$$G_{wy}(s) = C_{\mathrm{pre}}(s)G_{wz}(s),\; G_{uy}(s) = C_{\mathrm{pre}}(s)G_{uz}(s). \tag{27}$$

Next, substituting (25)-(27) into (20)-(21) of Theorem 1, after rewriting, yields

$$S_{y,1}(\omega) = \frac{C_{\mathrm{pre}}(j\omega)}{1 + L_1(\omega)}, \tag{28}$$

$$S_{y,n}(\omega) = \frac{-P(nj\omega)C_{\mathrm{pos}}(nj\omega)H_n(\omega)C_{\mathrm{pre}}(nj\omega)}{1 + L_{\mathrm{bl}}(nj\omega)} \cdots S_{y,1}(\omega)e^{j(n-1)\angle S_{y,1}(\omega)} \; \forall n \neq 1. \tag{29}$$

with

$$L_1(\omega) \coloneqq P(j\omega)C_{\mathrm{pos}}(j\omega)\big[C_{\mathrm{par}}(j\omega) + H_1(\omega)\big]C_{\mathrm{pre}}(j\omega), \tag{30}$$

$$L_{\mathrm{bl}}(s) \coloneqq P(s)C_{\mathrm{pos}}(s)\big[C_{\mathrm{par}}(s) + R_{\mathrm{bl}}(s)\big]C_{\mathrm{pre}}(s). \tag{31}$$

In a similar manner, substituting (25)-(28) into (23)-(24) of Theorem 1, after rewriting, yields

$$S_{z,1}(\omega) = \frac{1}{1+L_1(\omega)}, \tag{32}$$

$$S_{z,n}(\omega) = \frac{-L_n(\omega)}{1+L_{\text{bl}}(nj\omega)} S_{z,1}(\omega) e^{j(n-1)\angle S_{z,1}(\omega)} \; \forall n \neq 1, \tag{33}$$

$$L_n(\omega) := P(nj\omega) C_{\text{pos}}(nj\omega) H_n(\omega) \cdot \cdots \\ C_{\text{pre}}(j\omega) e^{j(n-1)\angle C_{\text{pre}}(j\omega)} \; \forall n \neq 1. \tag{34}$$

As expected, the HOSISFs in (32)-(33) are equivalent to the ones earlier reported in [8, Th. 2].

V. Numerical Computation of Pseudosensitivity

In this section we propose a numerical algorithm to compute the pseudosensitivity in (16) using Theorem 1, based on an FRF of LTI system G. To compute the performance output using Theorem 1 for a certain input frequency ω, information of LTI system G is required at integer-multiple frequencies of the input frequency, as can be seen from (24). Therefore, we assume from here that the FRF is available at a linearly-spaced grid of frequencies $\omega \in [\omega_1, \omega_2, \ldots, \omega_M]$, $M \in \mathbb{N}$, in such a way that $\omega_k = k\omega_1 \forall k \in [1, M]$. Hereby it is assured that, for any input frequency ω_k, information of system G is available at integer-multiples of ω_k (at least up to the highest available frequency ω_M). Even though it is outside the scope of this letter, we want to point the reader to, e.g., [3], for more information on how such a linearly-spaced FRF can be obtained with only a limited amount of measurement data.

Next, consider a sinusoidal input as in (15), with any input frequency ω_k. To compute the pseudosensitivity using (16), we require the periodic solution z_{s}. We cannot directly use Theorem 1 to compute this solution, because it requires information of LTI system G at frequencies larger than the frequency-range in which the FRF is available. Instead, we approximate periodic solution z_{s} by taking as many harmonics into account as is feasible based on the available FRF. Hereby, we can obtain the best possible approximation, as given by

$$\tilde{z}_{\text{s}}(t) = \hat{w} \sum_{n=1}^{n_{\max}} |S_{z,n}(\omega_k)| \sin\left(n(\omega_k t + \varphi_w) + \angle S_{z,n}(\omega_k)\right), \tag{35}$$

with $n_{\max} = \lfloor M/k \rfloor$.

To compute the pseudosensitivity using (16), we approximate the maximum absolute value of periodic solution $\tilde{z}_{\text{s}}$ by evaluating the solution at a finite set of time-instants

$$\tilde{t} = \{t_1, t_2, \ldots, t_P\}, \tag{36}$$

where $t_i = \frac{(i-1)}{P} T$ and $P \in \mathbb{N}$ is the number of time-instants in one time-period T. In that manner we can approximate the pseudosensitivity, based on a plant FRF, by

$$\left|\tilde{S}_\infty(\omega_k)\right| = \frac{\max_{t \in \tilde{t}} |\tilde{z}_{\text{s}}(t)|}{\hat{w}}, \tag{37}$$

with $\tilde{z}_{\text{s}}(t)$ as in (35) and $\tilde{t}$ as in (36). Note that, without loss of generality, we can assume $\hat{w} = 1$. Namely, both the numerator and denominator of (37) scale proportionally with $\hat{w}$. Similarly, we can assume $\varphi_w = 0$, because changing the input phase only shifts the performance output $\tilde{z}_{\text{s}}$ in time, meaning that the maximum over one period T stays the same.

The remaining question is how the number of time-instants P should be chosen. A larger P yields a more accurate approximation of the maximum absolute value, but also requires more computation time. Therefore, we desire a P which is as small as possible, but large enough to get an accurate approximation. According to the Nyquist-Shannon sampling theorem, at least two sample points are needed per period of a harmonic to be able to detect it. Therefore, to be able to detect the highest harmonic in the solution, we require $P \geq 2n_{\max}$. However, to more accurately reconstruct the maximum absolute value, one could for example also choose $P \geq 10n_{\max}$.

A MATLAB-based implementation of the algorithm can be found in [15], which also contains a demonstration of the algorithm on an example system. The FRF in the example contains $M = 4000$ frequencies. Furthermore, $P = 100n_{\max}$ has been chosen. To give an indication of the computation time, the algorithm takes in the order of 20 seconds to execute on a regular laptop with an Intel Core Ultra 7 Processor 155H. The interested reader is also referred to illustrative examples in the earlier works [7], [8]. Although our work can cover a broader class of systems, the pseudosensitivities obtained in those examples are essentially the same as the ones following from the proposed algorithm.

VI. Conclusion

In this letter, we developed a method to predict the output of general closed-loop systems containing a nonlinear reset control element, given a sinusoidal input. The considered class of reset control systems unifies and extends upon all classes considered in the existing literature. The higher-order sinusoidal-input sensitivity functions that are used to compute the output, can be obtained based solely on a frequency-response function of the system's LTI part. Therefore, the output can be predicted without requiring a parametric model of the LTI part. Based on the output, the developed numerical algorithm can compute the pseudo-sensitivity in an accurate and computationally efficient manner. Hereby, it is also possible to trade-off accuracy for computational efficiency when desired. Since the pseudo-sensitivity has similarity to the closed-loop sensitivity that is often used for LTI control design, this makes the design approach for reset controllers rather intuitive. We hope that the provided numerical algorithm can boost wider adoption of this design technique.

In future work, we will derive rigorous conditions under which modeling the reset element as in Fig. 1 is valid. Furthermore, we want to extend the prediction method to reset elements with other reset conditions.

Appendix
Technical Proof of Theorem 1

Consider the sinusoidal input in (15), which can be alternatively written as $w(t) = |W(j\omega)| \sin(\omega t + \angle W(j\omega))$ with

$$W(j\omega) = \hat{w} e^{j\varphi_w}. \tag{38}$$

Given that the system is sinusoidal-input convergent, the signals u, y, and z converge to a $\frac{2\pi}{\omega}$-periodic solution with a zero-mean, which can be described by the Fourier series

$$u(t) = \sum_{n=1}^{\infty} |U_n(\omega)| \sin\big(n\omega t + \angle U_n(\omega)\big), \tag{39}$$

$$y(t) = \sum_{n=1}^{\infty} |Y_n(\omega)| \sin\big(n\omega t + \angle Y_n(\omega)\big), \tag{40}$$

$$z(t) = \sum_{n=1}^{\infty} |Z_n(\omega)| \sin\big(n\omega t + \angle Z_n(\omega)\big), \tag{41}$$

respectively. Note that the constant offset terms ($n = 0$) can be omitted in (39)-(41) because they have a zero-mean.

Next, in steps 1 till 4 we derive the HOSISFs as given in (20), (21), (23), and (24), respectively. Finally, in step 5 we derive the periodic solutions to which the reset element's input in (19) and the performance output in (22) converge.

STEP 1: First, we derive Y_1 as a function of external input W. This can be done by balancing the first harmonic using (17)-(18), resulting in

$$Y_1(\omega) = G_{wy}(j\omega)W(j\omega) + G_{uy}(j\omega)U_1(\omega), \tag{42}$$

When the condition in (3) holds, then modeling the reset element as in Fig. 1 allows for substituting (13) in (42), which after rewriting yields

$$Y_1(\omega) = S_{y,1}(\omega)W(j\omega), \tag{43}$$

with $S_{y,1}$ as in (20).

STEP 2: Second, we derive Y_n, for all $n \neq 1$, as a function of external input W. This can be done by balancing the higher harmonics using (17)-(18), resulting in

$$Y_n(\omega) = G_{uy}(nj\omega)U_n(\omega)\,\forall n \neq 1. \tag{44}$$

Substituting (14) in (44), and rewriting, yields

$$Y_n(\omega) = \frac{G_{uy}(nj\omega)H_n(\omega)Y_1(\omega)e^{j(n-1)\angle Y_1(\omega)}}{1 - G_{uy}(nj\omega)R_{\mathrm{bl}}(nj\omega)}\,\forall n \neq 1. \tag{45}$$

Substituting (43) in (45) results in

$$Y_n(\omega) = S_{y,n}(\omega)W(j\omega)e^{j(n-1)\angle W(j\omega)}\,\forall n \neq 1, \tag{46}$$

with $S_{y,n}$ as in (21).

STEP 3: Third, we derive Z_1 as a function of external input W. This can be done by balancing the first harmonic using (17)-(18), resulting in

$$Z_1(\omega) = G_{wz}(j\omega)W(j\omega) + G_{uz}(j\omega)U_1(\omega). \tag{47}$$

Substituting (43) and (13) in (47), yields

$$Z_1(\omega) = S_{z,1}(\omega)W(j\omega), \tag{48}$$

with $S_{z,1}$ as in (23).

STEP 4: Fourth, we derive Z_n, for all $n \neq 1$, as a function of external input W. This can be done by balancing the higher harmonics using (17)-(18), resulting in

$$Z_n(\omega) = G_{uz}(nj\omega)U_n(\omega)\,\forall n \neq 1. \tag{49}$$

Substituting (43) and (46) in (14) results in

$$U_n(\omega) = \Big[H_n(\omega)S_{y,1}(\omega)e^{j(n-1)\angle S_{y,1}(\omega)} + \cdots R_{\mathrm{bl}}(nj\omega)S_{y,n}(\omega)\Big]W(j\omega)e^{j(n-1)\angle W(j\omega)}\,\forall n \neq 1. \tag{50}$$

Substituting (21) in (50), and rewriting, yields

$$U_n(\omega) = \frac{H_n(\omega)S_{y,1}(\omega)e^{j(n-1)\angle S_{y,1}(\omega)}}{1 - G_{uy}(nj\omega)R_{\mathrm{bl}}(nj\omega)} \cdots W(j\omega)e^{j(n-1)\angle W(j\omega)}\,\forall n \neq 1. \tag{51}$$

Substituting (51) in (49) results in

$$Z_n(\omega) = S_{z,n}(\omega)W(j\omega)e^{j(n-1)\angle W(j\omega)}\,\forall n \neq 1, \tag{52}$$

with $S_{z,n}$ as in (24).

STEP 5: By substituting (38), (43), and (46) into (40), after rewriting, we obtain (19). In a similar manner, by substituting (38), (48), and (52) into (41), after rewriting, we obtain (22). This concludes the proof.

Acknowledgment

The authors thank D. Caporale, Y. Liu, and B. Cheizoo for fruitful collaborations which led to this letter.

References

[1] F. Lamnabhi-Lagarrigue et al., "Systems & control for the future of humanity, research agenda: Current and future roles, impact and grand challenges," *Annu. Rev. Control*, vol. 43, pp. 1–64, Apr. 2017.
[2] G. F. Franklin, J. D. Powell, and A. E. Emami-Naeini, *Feedback Control of Dynamic Systems*, 7th ed. London, U.K.: Pearson, 2015.
[3] R. Pintelon and J. Schoukens, *System Identification: A Frequency Domain Approach*, 2nd ed. Hoboken, NJ, USA: Wiley/IEEE Press, 2012.
[4] J. Freudenberg, R. Middleton, and A. Stefanpoulou, "A survey of inherent design limitations," in *Proc. Amer. Control Conf.*, vol. 5, 2000, pp. 2987–3001.
[5] O. Beker, C. Hollot, and Y. Chait, "Plant with integrator: An example of reset control overcoming limitations of linear feedback," *IEEE Trans. Autom. Control*, vol. 46, no. 11, pp. 1797–1799, Nov. 2001.
[6] G. Zhao, D. Nešić, Y. Tan, and C. Hua, "Overcoming overshoot performance limitations of linear systems with reset control," *Automatica*, vol. 101, pp. 27–35, Mar. 2019.
[7] N. Saikumar, K. Heinen, and S. H. HosseinNia, "Loop-shaping for reset control systems: A higher-order sinusoidal-input describing functions approach," *Control Eng. Pract.*, vol. 111, Jun. 2021, Art. no. 104808.
[8] D. Caporale, L. F. van Eijk, N. Karbasizadeh, S. Beer, D. Kostić, and S. H. HosseinNia, "Practical implementation of a reset controller to improve performance of an industrial motion stage," *IEEE Trans. Control Syst. Technol.*, vol. 32, no. 4, pp. 1451–1462, Jul. 2024.
[9] L. F. van Eijk, Y. Liu, X. Zhang, D. Kostić, and S. H. HosseinNia, "A nonlinear integrator based on the first-order reset element," *IFAC-PapersOnLine*, vol. 58, no. 7, pp. 382–387, 2024.
[10] N. Karbasizadeh and S. H. HosseinNia, "Continuous reset element: Transient and steady-state analysis for precision motion systems," *Control Eng. Pract.*, vol. 126, Sep. 2022, Art. no. 105232.
[11] H. K. Khalil, *Nonlinear Systems*, 3rd ed. London, U.K.: Pearson, 2002.
[12] Y. Guo, Y. Wang, and L. Xie, "Frequency-domain properties of reset systems with application in hard-disk-drive systems," *IEEE Trans. Control Syst. Technol.*, vol. 17, no. 6, pp. 1446–1453, Nov. 2009.
[13] L. F. van Eijk, D. Kostić, M. Khosravi, and S. H. HosseinNia, "Higher order sinusoidal-input describing function analysis for a class of multiple-input multiple-output convergent systems," *IEEE Trans. Autom. Control*, vol. 70, no. 1, pp. 673–680, Jan. 2025.
[14] A. A. Dastjerdi, A. Astolfi, N. Saikumar, N. Karbasizadeh, D. Valério, and S. H. HosseinNia, "Closed-loop frequency analysis of reset control systems," *IEEE Trans. Autom. Control*, vol. 68, no. 2, pp. 1146–1153, Feb. 2023.
[15] L. F. van Eijk, D. Kostić, and S. H. HosseinNia. "Code accompanying the article." Accessed: Jun. 16, 2025. [Online]. Available: https://github.com/lukevaneijk/pseudoSensReset